J. Am. Soc. Mass Spectrom. (2019) 30:1190–1198
DOI: 10.1007/s13361-019-02191-w

RESEARCH ARTICLE

Standard Proteoforms and Their Complexes for Native Mass Spectrometry

Luis F. Schachner, Ashley N. Ives, John P. McGee, Rafael D. Melani, Jared O. Kafader, Philip D. Compton, Steven M. Patrie, Neil L. Kelleher

Departments of Chemistry and Molecular Biosciences, the Chemistry of Life Processes Institute, and the Proteomics Center of Excellence, Northwestern University, 2170 Tech Dr., Silverman Hall, Evanston, IL 60208, USA

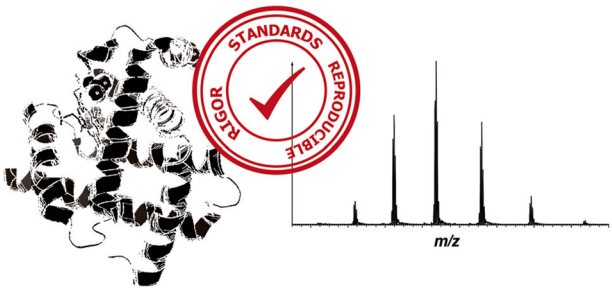

Abstract. Native mass spectrometry (nMS) is a technique growing at the interface of analytical chemistry, structural biology, and proteomics that enables the detection and partial characterization of non-covalent protein assemblies. Currently, the standardization and dissemination of nMS is hampered by technical challenges associated with instrument operation, benchmarking, and optimization over time. Here, we provide a standard operating procedure for acquiring high-quality native mass spectra of 30–300 kDa proteins using an Orbitrap mass spectrometer. By describing reproducible sample preparation, loading, ionization, and nMS analysis, we forward two proteoforms and three complexes as possible standards to advance training and longitudinal assessment of instrument performance. Spectral data for five standards can guide assessment of instrument parameters, data production, and data analysis. By introducing this set of standards and protocols, we aim to help normalize native mass spectrometry practices across labs and provide benchmarks for reproducibility and high-quality data production in the years ahead.

Keywords: Native mass spectrometry, Native top-down mass spectrometry, Proteoforms, Multi-proteoform complexes, Standards, Rigor and reproducibility

Received: 3 December 2018/Revised: 4 March 2019/Accepted: 11 March 2019/Published Online: 8 April 2019

Introduction

Native mass spectrometry (nMS) has emerged as a valuable approach to complement the field of structural biology [1–3]. The technique utilizes "native"—or non-denaturing and non-reducing—buffer conditions during the electrospray ionization process which helps preserve the primary and quaternary compositions of proteins and their complexes for subsequent MS analysis [4, 5]. nMS offers unique advantages to structural biologists because modern mass analyzers provide highly accurate mass measurements of the intact protein targets and any products that result from subsequent rounds of activation (i.e., tandem mass spectrometry, MS^n) [6, 7]. The gas-phase activation of protein complexes that yield sequence-informative product ions, or native top-down mass spectrometry (nTDMS) [8–10], provides insights into the identity of protein subunits, their stoichiometry and even interaction sites in a complex, and can help discover and characterize binding of many classes of cofactors (e.g., metals, ligands, reaction products or substrates, drug fragments) [11–14]. Also for the characterization of protein-subunits, the resolution of discrete molecular proteoforms that arise from polymorphisms, RNA splicing variants, and post-translational modifications (PTMs) allows protein assemblies to be viewed as multi-proteoform complexes (MPCs), in which differentially modified subunits combine into many possible complexes, each with potentially discrete functions [15, 16].

Electronic supplementary material The online version of this article (https://doi.org/10.1007/s13361-019-02191-w) contains supplementary material, which is available to authorized users.

Correspondence to: Neil Kelleher; *e-mail:* n–kelleher@northwestern.edu

Over the last several years, numerous technological advancements have driven the increased application of nMS. MS-compatible sample handling techniques (e.g., membrane proteins embedded within nanodiscs [17], amphipols [18], and detergent micelles [19, 20]) have facilitated mechanistic studies on previously inaccessible membrane protein complexes. Innovations in non-denaturing chromatography (e.g., online size-exclusion [21, 22] and native GELFrEE [23]) have assisted in the characterization of complex biopharmaceuticals [24], the separation of endogenous protein complexes [23], and increased the dynamic range of nMS in omics-level interrogations on macromolecular assemblies [22, 25]. Also, data processing and bioinformatics resources now permit the precise MS deconvolution of high mass assemblies (e.g., protein deconvolution, MagTran, UniDec) [26, 27], omics-level prediction of MPCs [16, 28], and the automated interpretation of tandem MS data (e.g., ProSight Lite, ProSightPC, TDValidator, mMass) [29, 30]. Plus, the development in hybrid mass analyzer technologies [31–33], in particular time-of-flight (TOF) [34–36] and Fourier Transform (FT), including ion cyclotron resonance (ICR) and Orbitrap [37, 38], have expanded the applicability of nMS to analytes with wide-ranging size, shape, complexity, and throughput. For example, ion-mobility has been widely applied to study biomolecule conformations in the gas-phase [39–42], and novel instrument designs, including the infinity cell for ICR analyzers [43, 44] and the UHMR for the Orbitrap [45], have improved sensitivity and resolving power for high-mass biomolecules, even for protein assemblies over 1 MDa such as viral capsids and ribosomes [46, 47]. Additionally, different MS^n techniques, including high-energy collision dissociation (HCD), source-induced dissociation (SID), surface-induced dissociation, ultraviolet photo-dissociation (UVPD), electron capture dissociation (ECD), and electron transfer dissociation (ETD) serve complementary roles in the gas-phase characterization of native proteins and larger assemblies [8, 48–51].

Despite significant achievements within many labs using nMS over the past decade, the development of universal standards would help set a baseline of quality for newcomers and of reproducibility for expert groups, as recommended by the NIH, NSF, and other regulatory bodies [52–55]. While many protocols have been published on nMS methodology in select systems, they often describe the analysis of native proteins or assemblies not readily available to the research community and do not detail the optimization of acquisition parameters [56–59]. Moreover, the complex instrumentation and technical difficulty of nMS are barriers in disseminating the technology more widely. A valuable addition to the field is a tutorial that demonstrates the analysis of commercial proteins that are reasonably stable and broadly accessible. Herein, we present standard samples and an operating procedure for a Thermo Fisher Q Exactive Orbitrap HF with Extended Mass Range (QE-EMR) and for a Thermo Fisher Q Exactive Orbitrap with Ultra High Mass Range (UHMR). The Orbitrap mass analyzer [38, 60] represents a growing platform for nMS analysis. We include representative spectra and raw data for the proposed protein standards and provide a troubleshooting guide for common challenges encountered. We also outline parameters for the ion source, ion optics, collision cells, and vacuum pressures that have been optimized for high signal intensity and signal-to-noise ratio (SNR) using Orbitrap technology across the 30–300 kDa molecular weight range.

Experimental Section

Fig. 1 contains a workflow of the proposed procedure and can help readers navigate this document.

Reagents

A complete list of part numbers and vendor information for standards, key reagents, solvents, and other resources used are available in Table S1.

Preparation of Solvents and Standards

Stock solutions (1 M) of LC-MS grade ammonium acetate (Sigma Aldrich) was prepared in LC/MS Grade Optima™ Water (Thermo Fisher Scientific) and then filtered using a 0.2 μm pore size Nalgene™ Rapid-Flow™ sterile disposable filters (Fisher Scientific). Protein stock solutions (10 mg/mL) were prepared in LC/MS Grade Optima™ Water (Fisher Scientific) with aliquots flash frozen and stored at − 80 °C. Protein stocks were desalted and solvent exchanged into 150 mM ammonium acetate [61] using Amicon Ultra-0.5-mL centrifugal filters with 10–50 kDa molecular weight cut-offs, depending on protein molecular weight. First, the filter device was equilibrated with 500 μL of 150 mM ammonium acetate and spun for 5 min at 12,000 ×*g*. The protein sample was then dispensed into the filter device, up to a total volume of 500 μL, and spun for 5 min at 12,000 ×*g* or until the sample was concentrated to a volume of 100 μL or less. Ten to 15 consecutive washes were performed by adding enough ammonium acetate (150 mM) for a total volume of 500 μL and spun at 12,000 ×*g* for 5 min. Sample was pipetted carefully out of the device and diluted to the initial volume with 150 mM ammonium acetate. The final analytical samples were prepared at a concentration of 10 pmol/μL in 150 mM ammonium acetate. While several methods for buffer exchanging and desalting are compatible with nMS, we have found that the ability to increase the number of washes using the Amicon spin filters provides flexibility in the extent of desalting — which depends on the sample type and original buffer conditions. Poor washing or desalting results in salt adduction and non-covalent adducts; we thus recommend 10 to 15 consecutive washes as this will ensure that the sample quality is optimal for nMS after exchange from most biochemical buffers.

MS and Ion Source Parameters

A custom Thermo Fisher Q Exactive Orbitrap HF MS with Extended Mass Range (QE-EMR) [8] and a commercially

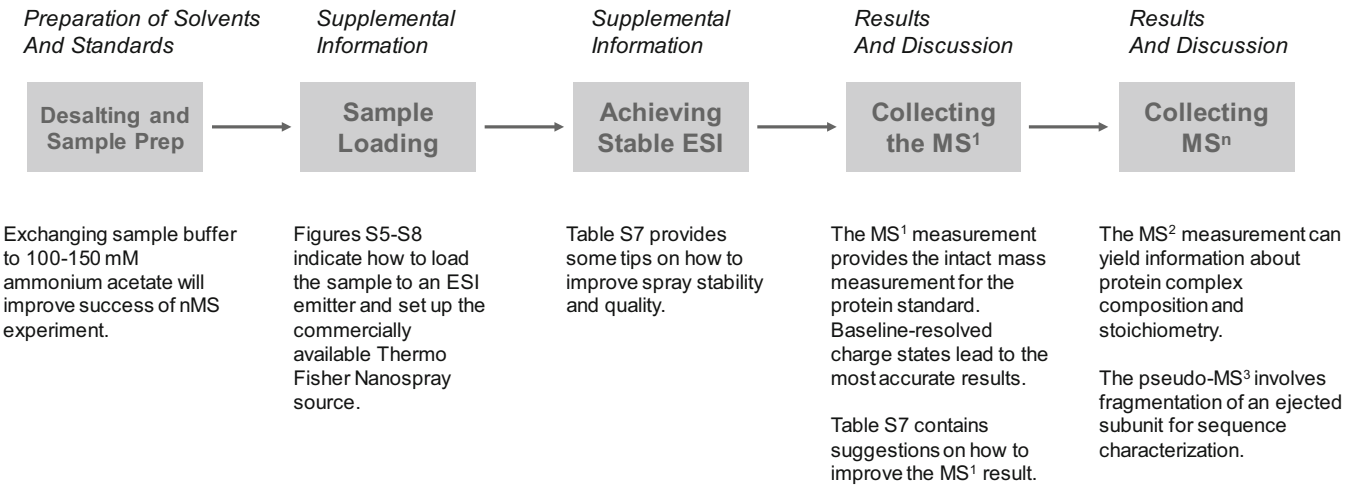

Figure 1. Workflow of the proposed standard operating procedure for native mass spectrometry. Text in gray boxes denotes the specific step in the procedure. Text at the top of the boxes indicates the location of that step within this document; the text at the bottom of each box elaborates on the specific step

available Thermo Fisher Q Exactive Orbitrap MS with Ultra High Mass Range (UHMR) were used. Suggested values for key instrument tuning and data acquisition parameters are provided in Table S2. The QE-EMR and UHMR mass spectrometers were mass calibrated for extended mass range mode using a 50 mg/mL Cesium Iodide solution in water at an HCD pressure regulator setting of 4 V. Table S2 contains the UHV pressures that correspond to each regulator pressure setting on the QE-EMR and UHMR instruments. The effect of pressure and collision voltage settings on the CsI spectrum have been discussed previously [56]. nMS analyses were performed on commercial Nanospray and Nanospray Flex Ion Sources with a static NSI probe (Thermo Fisher Scientific) as well as a capillary-based ion source described previously [62]. Detailed assembly and sample loading instructions for all sources are available as supplemental information. The sources were held at a voltage of + 0.9–2.0 kV and the inlet capillary of the MS was heated to 330 °C (QE-EMR) or 300 °C (UHMR). Back pressure can be applied to the Thermo Fisher Nanospray (Flex) Ion Source to initially stabilize the electrospray signal or to overcome clogging of the emitter, which is commonly observed for larger proteoforms or complexes.

Data Analysis

Spectra were manually inspected and analyzed using Thermo Xcalibur 4.0 Qual Browser (Thermo Fisher Scientific, Inc.) and assembled into a figure for publication using Adobe Illustrator CC 2015.3. Table S3 contains spectral parameter averages and ranges derived for the indicated base peak(s), as well as values for resolution, baseline intensity, and noise intensity. SNR was calculated by subtracting the baseline intensity (B) from the signal intensity (NL) and the noise (N) intensity, and dividing: SNR = (N − B) / (N − B). The mass spectra data files (.RAW) of the protein standards measured on the QE-EMR are publicly available online at https://massive.ucsd.edu under Accession Number MSV000083343. Fragmentation data were analyzed using ProSight Lite [30] with a 25 ppm error cutoff for identified fragments.

Results and Discussion

Five protein systems were used to evaluate instrument performance across several dimensions. Bovine carbonic anhydrase (CA, 29.1 kDa) was chosen as representative of monomeric and small proteins and can aid in the evaluation of labile cofactors such as bicarbonate or metal ions. An antibody was chosen as a standard given the significant literature precedent in the analysis of antibodies by nMS [63–66]; thus, SILu antibody (147 kDa) provides a Biopharma-relevant sample type in a standard panel and assists in the diagnosis of mass accuracy and resolution of glyco-proteoforms. Finally, tetrameric pyruvate kinase from rabbit muscle (PK, 230 kDa), tetrameric alcohol dehydrogenase from baker's yeast (ADH, 148 kDa), and dimeric enolase from baker's yeast (93 kDa) are proposed as standards in the analysis of non-covalent protein assemblies and their dissociated subunits and to test ion transmission efficiency at high *m*/*z*.

Representative spectra acquired on the QE-EMR are provided in Figure 2 for this set of standard proteins and complexes. Table S3 contains values or ranges for signal intensity, signal-to-noise ratio (SNR), and resolution for the indicated base peaks derived from multiple replicates of each standard on the separate ion sources. Overall, these standards yield an average NL of 9.47×10^5 and average SNR of 1447 ($N = 16$; Standard Error = ± 769). The reported values serve to illustrate typical ranges that can be expected in the analysis of the standards. In our hands, the variability in these ranges stems from spray instability and from non-uniform tip sizes. Tables S4–S5 contain deconvoluted average masses, and mass errors relative to the theoretical masses of the standards.

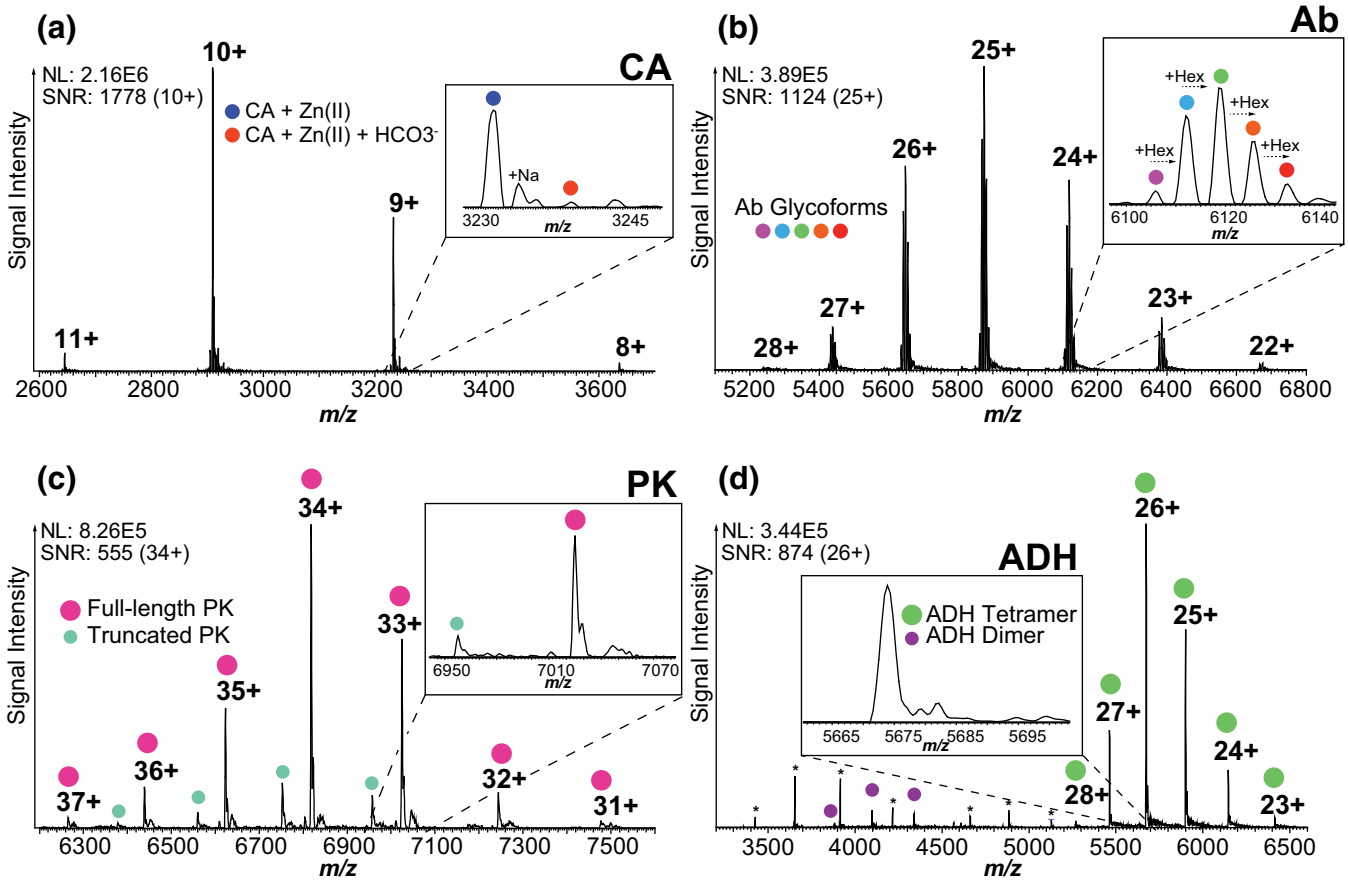

Figure 2. Representative native mass spectra acquired on the QE-EMR for carbonic anhydrase (**a**), SILu antibody (**b**), pyruvate kinase (**c**), and alcohol dehydrogenase (**d**). NL indicates signal intensity and SNR the signal-to-noise ratio for the most abundant charge state. The insets show a zoom-in of the indicated charge state. Asterisks in panel **1d** denote protein impurities in the sample

Table 1 contains the annotations of post-translational modifications, sequence variations, and cofactors considered in the mass calculations. The average mass error in the measurement of the standards was ± 1.6 Da (12.2 ppm). These values can serve as criteria for assessing the quality or reproducibility of the data, and for tracking instrument calibration or performance.

Figure 2a contains a native mass spectrum of bovine carbonic anhydrase II, showing four charge states (8–11+) spanning the *m/z* range of 2600–3700. The observed charge state distribution, centered at high *m/z* with few charge states, is consistent with the model advanced by Fernandez de la Mora, which estimates the maximum charge of globular protein ions that retain their native structures [4]. The inset around the 9+ charge state illustrates base-line resolution and reflects the major species that is routinely observed by nMS of CA. The most abundant proteoform corresponds to CA with the initiator methionine removed (MetOFF), N-terminal acetylation (NtAc) of the adjacent Ser, and a single bound Zn (II) ion. The assigned 2+ oxidation state for the zinc ion, yielding a theoretical mass for CA of 29,088.0 Da, is most consistent with the experimentally derived result (29,087.5 Da ± 0.4). The molecular ion at < 5% relative intensity, indicated in red, corresponds to the observed base peak with an addition of one + 62 Da adduct peaks asserted here to be a bicarbonate (HCO_3^-) ion ionically bound to the protein. The observation of Zn (II) bound to CA along with bicarbonate, its natural reaction product, is in accordance with the known crystal structure and enzymatic activity [67].

Table 1. PTMs, sequence variations, and cofactors considered in theoretical average masses of Table S4. MetOFF? indicates whether the initiator methionine has been removed

Standard	MetOFF?	PTM/cofactor	Sequence variations
CA	Yes	NtAc (42.0 Da) Zn (II) (63.7 Da)	–
SILu	Yes	Major glycoform: 2× Pyroglutamate (Q), G0F+G1F (1607.47 + 1445.33 Da)	–
PK	Yes	Beta-mercaptoethanol (76.1 Da)	S ➔ A (− 16.0 Da)
ADH	Yes	NtAc (42.0 Da) 2× Zn (II) (127.4 Da)	I ➔ V (− 14.0 Da)
EN	Yes	–	I ➔ V (− 14.0 Da)

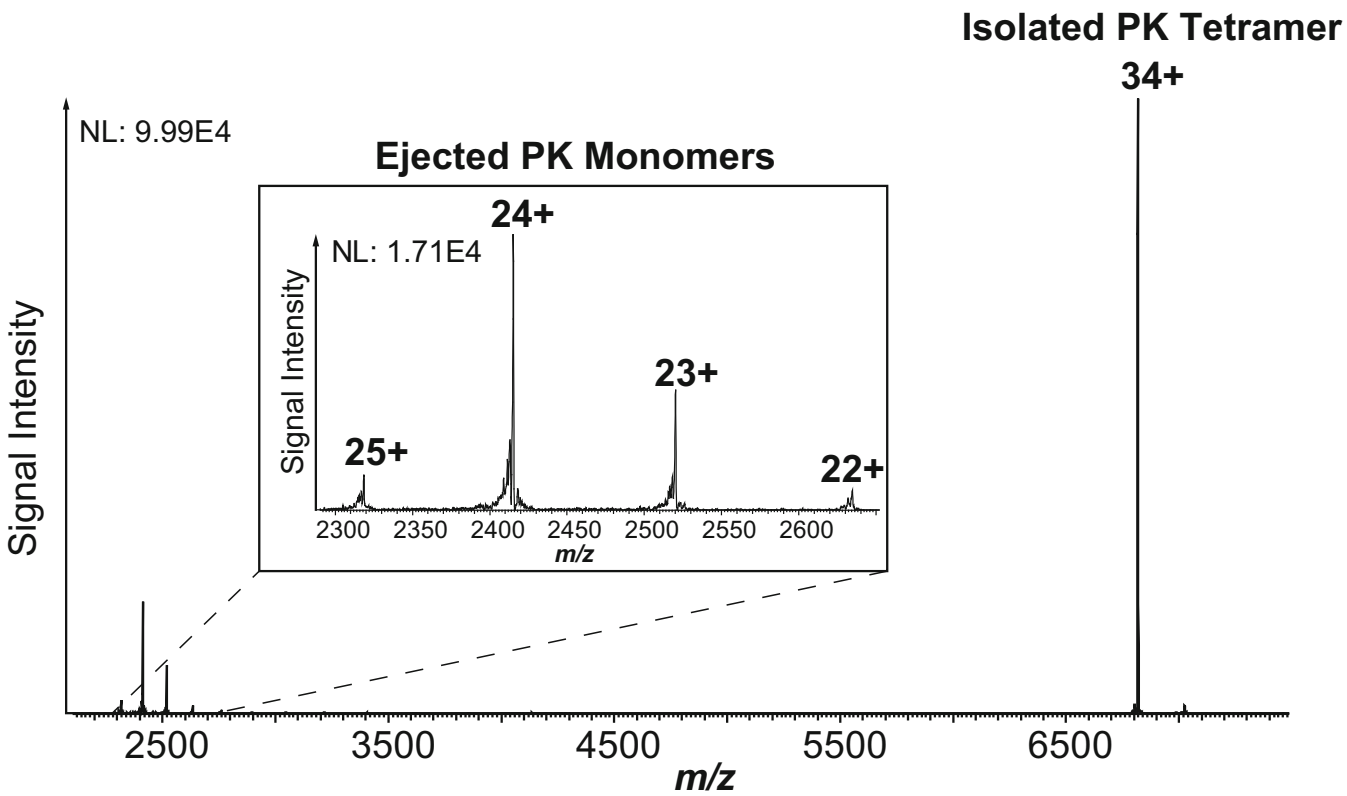

Figure 3. MS^2 spectrum showing the isolated 34+ charge state of the PK tetramer that was activated to release four charge states (22–25+) shown in the inset to span the range of 2300–2650 *m/z*, that correspond to the ejected PK subunits, with an observed average mass of 57,941.2 Da (theoretical average mass: 57,942.8 Da). In order to achieve this spectral result on the QE-EMR, the 34+ charge state (6817 *m/z*) of the full-length PK tetramer was isolated with a 10 *m/z* window and collisionally activated in the HCD cell (120 V) at a pressure regulator setting of 2 V. The resultant MS^2 is an average of five scans of ten microscans each

The spectrum in Figure 2b of SILu antibody, shows a charge state distribution (22–28+) that spans the range of 5000–7000 *m/z*. The inset highlights five known glyco-proteoforms of SILu (Table S5) that differ in mass by ~ 162 Da, consistent with increments in hexose content. The mass of the observed SILu glyco-proteoforms matched to their theoretical masses with an average standard error of ± 0.5 Da (3.6 ppm) thus serving as a benchmark expectation for mass accuracy in this high *m/z* region of the spectrum.

Shown in Figure 2c is a native mass spectrum of the pyruvate kinase tetramer from rabbit muscle, containing two major charge state envelopes that range from 6000 to 7500 *m/z* and span the 31–37+ protonation states; these correspond to two multi-proteoform complexes (MPCs) of PK tetramers. The mass of the most abundant PK multi-proteoform complex (MPC) corresponds to the PK tetramer with each subunit being MetOFF, followed by NtAc of the Ser residue, a S400A sequence variant, and a covalent β-mercaptoethanol (BME) modification at Cys165 on two subunits already present in several commercial stock samples we have tested over the past few years [16]. The second PK MPC contains three subunits as described above, and one PK proteoform that consists of residues 23–531 of the full-length proteoform, resulting from an endogenous N-terminal cleavage after Met22 [16]. The inset shows that the full-length PK tetramer has a higher-mass shoulder peak that corresponds to the PK tetramer with additional covalent BME modifications on the other two subunits.

While PK provides a robust standard for assessing the transmission of ions up to 8000 *m/z*, a standard is needed, namely alcohol dehydrogenase from yeast (Figure 2d), that can probe the transmission of non-covalent assemblies in the *m/z* range compatible with instruments designed for analysis < 6000 *m/z*. The major charge envelope centered around 5000–6600 *m/z* corresponds to the tetramer of ADH; the minor distribution in the range of 3200–4400 *m/z* corresponds in mass to the ADH dimer. Changes in the HCD pressure regulator setting can modulate the ratio of dimer to tetramer of ADH detected and can be a useful tool for optimizing this parameter. The inset contains a zoom-in of the 26+ charge state, highlighting the major tetramer species, characterized as a homotetramer of ADH subunits being MetOFF, followed by NtAc of the Ser residue, an I– > V sequence variation, and containing two Zn (II) cofactors per subunit [10, 68, 69]. A lower molecular weight alternative to ADH is the Enolase dimer (EN) from Baker's yeast, for which we present a native mass spectrum in Supplemental Figure 1. The major charge state distribution (22–18+) is centered around 4200–5200 *m/z* and corresponds to the dimer of the enzyme. Charge state deconvolution of the spectrum yields a mass of 93,343.2 ± 2.3 Da, which is − 1.4 Da

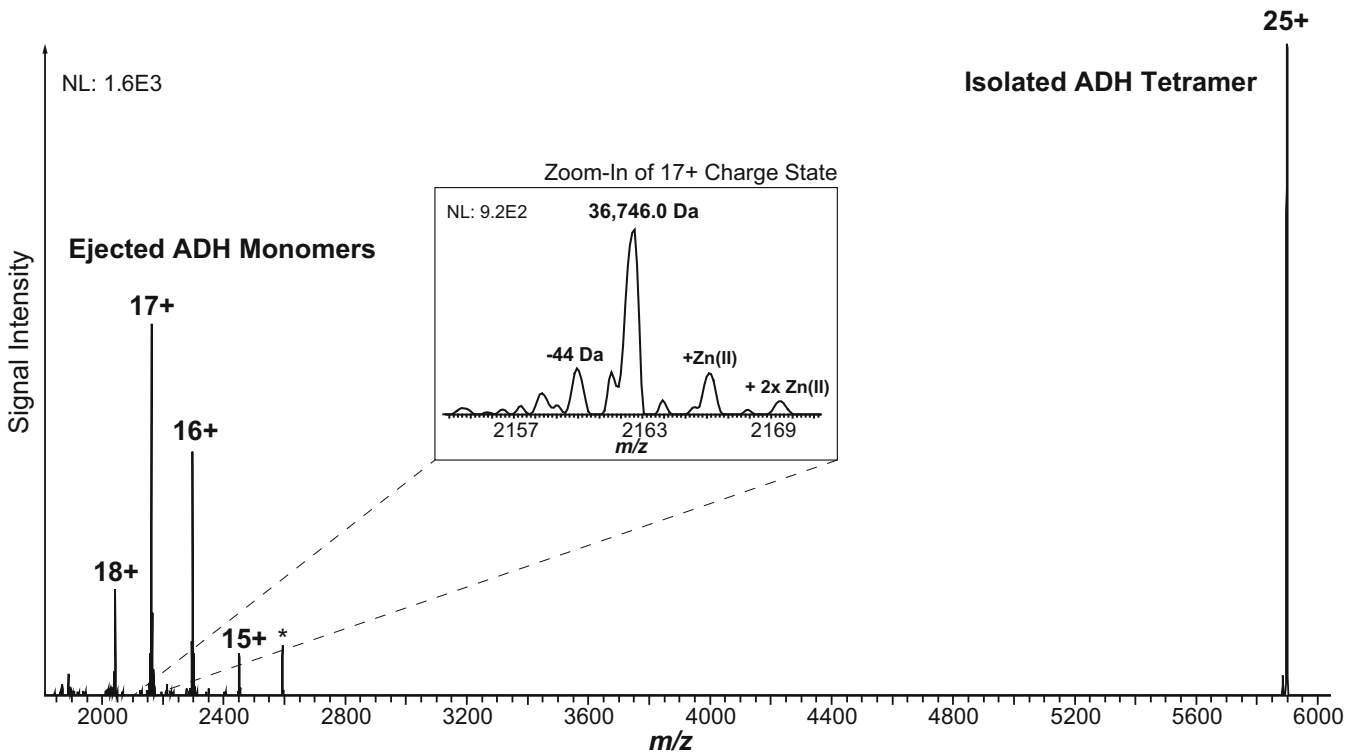

Figure 4. MS^2 spectrum showing the isolated 25+ charge state of the ADH tetramer that was activated to release the ejected ADH monomer charge state distribution (15–18+) in the range of 2000–2350 *m/z*, and yielding an observed average mass of 36,746.0 Da (theoretical average mass for Apo-ADH: 36,746.0 Da). The inset of the spectrum is a zoom-in of the 17+ charge state illustrating the ADH monomer bound to 1 or 2 Zn (II) ions. The inset also shows the presence of a – 44 Da mass shift from the base peak, consistent with previous reports of yeast ADH [69]. To achieve this spectral result on the QE-EMR, the 25+ charge state (5900 *m/z*) of the ADH tetramer was isolated with a 10 *m/z* window and collisionally activated in the HCD cell (175 V) at a pressure regulator setting of 2 V. The resultant MS^2 is an average of five scans of ten microscans each

from the theoretical mass of apo-EN, assuming cleavage of the initiator methionine and a known I– > V sequence variant [70].

ADH and PK standards are high *m/z* ions that can aid in the diagnosis of instrument transmission and MS-compatibility of experimental sample preparation protocols. For this purpose, SNR values can function as metrics of transmission efficiency and reproducibility, with the caveat that they are not to be interpreted as absolute measures of performance. For instance, in the case of the PK standard, even though its NL intensity values are high, ranging between 4.69×10^5 and 1.06×10^6 for all replicates, the corresponding SNR range, 155–831, is lower than that of the other standards. This apparent discrepancy likely results from inferior transmission and desolvation of large protein complexes through the instrument, causing higher noise and lowering the SNR. The NL values reported in the spectrum can differ between instrumental platforms, thus it is important to consider these values in conjunction with SNR, resolution, mass accuracy, and overall spectral quality in order to assess longitudinal performance of the nMS system.

We employed nTDMS to demonstrate standard instrumental parameters for the characterization of ejected proteoforms in the PK standard. Figure 3 contains the MS^2 spectrum of the unmodified PK monomer ejected from an isolated charge state of the PK tetramer (24+) using HCD activation energy, and Supplemental Figures S2 and S3 show the source dissociation followed by top-down backbone fragmentation of the ejected PK monomer. This experiment can be described as nTDMS because the subunit dissociated at the source from the native complex is fragmented to generate sequence-informative ions. The intensity of the isolated PK subunit that will be subjected to fragmentation, typically with an NL value > 2×10^3 at an FT resolution setting of 120,000 at 400 *m/z*, can serve as a diagnostic of ion transmission efficiency, as low precursor intensity and subsequent poor fragmentation may indicate malfunction or dirtying of the ion optics.

As a demonstration of a subunit-ejection experiment on a non-covalent protein complex, we provide Figure 4, which contains the MS^2 spectrum of the ADH monomer ejected from the 25+ tetramer charge state, demonstrating binding by up to two Zn (II) cofactors and the presence of an ADH proteoform with a − 44 Da shift [69]. Given that no sequence-informative ions are formed, this experiment does not technically fall under the category of top-down; however, the visualization of the ADH proteoforms with varying degrees of zinc-binding highlights the value of such an experiment for assigning complex stoichiometry and for partial proteoform characterization.

This standard operating procedure for nMS has been helpful in addressing typical analytical challenges in our setup

including low SNR, spray instability, and malfunction of the electrospray emitter. It has also proven useful for optimizing the collision voltages and pressure settings in the HCD cell for nTDMS. Moreover, the procedure provides a framework for longitudinal assessment of instrument performance over time and for technological development, given that the nMS tools are subject to problems not commonly seen in conventional proteomics assays that employ highly automated workflows. To test the validity of the protocol and the reproducibility of the measurements, we have performed this procedure using the proposed protein standards on a Thermo Fisher Q Exactive Orbitrap Ultra High Mass Range mass spectrometer (UHMR). The UHMR instrument has improved mass range and sensitivity for large molecular weight ions (up to ~75,000 *m/z* compared to 20,000 *m/z* on the QE-EMR), and enables isolation and tandem MS analysis of protein complexes at higher *m/z* values [45]. These modifications include: lowering the RF frequency of the instrument's ion guides for enhanced ion transmission; in-source trapping of ions for improved desolvation; and optimized transmission of high *m/z* ions from the C-trap into the Orbitrap [45]. The spectra acquired on the UHMR, presented in Figure S4, have SNR and resolution values comparable to those acquired on the QE-EMR (Table S6). Notably, even though SNR values are in the same order of magnitude for both data sets, the NL values for the UHMR spectra are lower than those for the QE-EMR spectra, highlighting that signal intensity should not be used as a standalone metric for data quality.

Finally, we provide Table S7, which contains a list of commonly observed problems and offers possible solutions, in the event that the same spectral quality is not readily achieved. The optimal parameters recommended in this article are instrument-dependent and may not yield the best results possible on every instrumental platform, as further optimization may be necessary using other available settings. However, given the benchmarking of key spectral metrics for the proposed standards, it will be interesting to see comparisons across instruments should this standard operating procedure be adopted by others.

Conclusions

Native MS offers a major way to increase researchers' success with intact mass spectrometry of their proteoforms and their complexes, even those of very high mass or complexity. The further adoption of nMS by researchers spanning multiple disciplines will necessitate adequate and standardized practices in sample preparation, instrument setup, and in data acquisition. We propose that this report serve as a benchmark for researchers at all levels of experience to asses and maintain consistent instrument performance and high-quality data production over time.

Acknowledgements

This work was supported by the National Institute of General Medical Sciences P41 GM108569 for the National Resource for Translational and Developmental Proteomics at Northwestern University. Research in this publication is also supported by a fellowship associated with the Chemistry of Life Processes Predoctoral Training Grant T32GM105538 at Northwestern University. LFS is a Gilliam Fellow of the Howard Hughes Medical Institute.

References

1. Loo, J.A.: Studying noncovalent protein complexes by electrospray ionization mass spectrometry. Mass Spectrom. Rev. **16**, 1–23 (1997)
2. Heck, A.J.R., van den Heuvel, R.H.H.: Investigation of intact protein complexes by mass spectrometry. Mass Spectrom. Rev. **23**, 368–389 (2004)
3. Hilton, G.R., Benesch, J.L.P.: Two decades of studying non-covalent biomolecular assemblies by means of electrospray ionization mass spectrometry. J. R. Soc. Interface. **9**, 801–816 (2012)
4. Fernandez de la Mora, J.: Electrospray ionization of large multiply charged species proceeds via Dole's charged residue mechanism. Anal. Chim. Acta. **2000**, 93–104 (1999)
5. Leney, A.C., Heck, A.J.: Native mass spectrometry: what is in the name? J. Am. Soc. Mass Spectrom. **28**, 5–13 (2017)
6. Benesch, J.L.P., Ruotolo, B.T., Simmons, D.A., Robinson, C.V.: Protein complexes in the gas phase: technology for structural genomics and proteomics. Chem. Rev. **107**, 3544–3567 (2007)
7. Sharon, M., Robinson, C.V.: The role of mass spectrometry in structure elucidation of dynamic protein complexes. Annu. Rev. Biochem. **76**, 167–193 (2007)
8. Belov, M.E., Damoc, E., Denisov, E., Compton, P.D., Horning, S., Makarov, A.A., Kelleher, N.L.: From protein complexes to subunit backbone fragments: a multi-stage approach to native mass spectrometry. Anal. Chem. **85**, 11163–11173 (2013)
9. Li, H., Nguyen, H.H., Ogorzalek Loo, R.R., Campuzano, I.D.G., Loo, J.A.: An integrated native mass spectrometry and top-down proteomics method that connects sequence to structure and function of macromolecular complexes. Nat. Chem. **10**, 139–178 (2018)
10. Zhang, H., Cui, W., Wen, J., Blankenship, R.E., Gross, M.L.: Native electrospray and electron-capture dissociation in FTICR mass spectrometry provide top-down sequencing of a protein component in an intact protein assembly. J. Am. Soc. Mass Spectrom. **21**, 1966–1968 (2010)
11. Kenney, G.E., Dassama, L.M.K., Pandelia, M.-E., Gizzi, A.S., Martinie, R.J., Gao, P., DeHart, C.J., Schachner, L.F., Skinner, O.S., Ro, S.Y., Zhu, X., Sadek, M., Thomas, P.M., Almo, S.C., Bollinger, J.M., Krebs, C., Kelleher, N.L., Rosenzweig, A.C.: The biosynthesis of methanobactin. Science. **359**, 1411–1416 (2018)
12. Skinner, O.S., Haverland, N.A., Fornelli, L., Melani, R.D., Do Vale, L.H.F., Seckler, H.S., Doubleday, P.F., Schachner, L.F., Srzentic, K., Kelleher, N.L., Compton, P.D.: Top-down characterization of endogenous protein complexes with native proteomics. Nat. Chem. Biol. **14**, 36–41 (2018)
13. Park, Y.J., Kenney, G.E., Schachner, L.F., Kelleher, N.L., Rosenzweig, A.C.: Repurposed HisC aminotransferases complete the biosynthesis of some methanobactins. Biochemistry. **57**, 3515–3523 (2018)
14. Sahasrabuddhe, A., Hsia, Y., Busch, F., Sheffler, W., King, N.P., Baker, D., Wysocki, V.H.: Confirmation of intersubunit connectivity and topology of designed protein complexes by native MS. Proc. Natl. Acad. Sci. **115**, 1268–1273 (2018)
15. Smith, L.M., Kelleher, N.L.: Consortium for TOP DOWN, P.: Proteoform: a single term describing protein complexity. Nat. Methods. **10**, 186–187 (2013)
16. Skinner, O.S., Havugimana, P.C., Haverland, N.A., Fornelli, L., Early, B.P., Greer, J.B., Fellers, R.T., Durbin, K.R., Do Vale, L.H.F., Melani, R.D., Seckler, H.S., Nelp, M.T., Belov, M.E., Horning, S.R., Makarov, A.A., LeDuc, R.D., Bandarian, V., Compton, P.D., Kelleher, N.L.: An informatic framework for decoding protein complexes by top-down mass spectrometry. Nat. Methods. **13**, 237 (2016)

17. Marty, M.T., Hoi, K.K., Gault, J., Robinson, C.V.: Probing the lipid annular belt by gas-phase dissociation of membrane proteins in nanodiscs. Angew. Chem. Int. Ed. **55**, 550–554 (2016)
18. Hopper, J.T.S., Yu, Y.T.-C., Li, D., Raymond, A., Bostock, M., Liko, I., Mikhailov, V., Laganowsky, A., Benesch, J.L.P., Caffrey, M., Nietlispach, D., Robinson, C.V.: Detergent-free mass spectrometry of membrane protein complexes. Nat. Methods. **10**, 1206 (2013)
19. Campuzano, I.D.G., Li, H., Bagal, D., Lippens, J.L., Svitel, J., Kurzeja, R.J.M., Xu, H., Schnier, P.D., Loo, J.A.: Native MS analysis of bacteriorhodopsin and an empty nanodisc by orthogonal acceleration time-of-flight, Orbitrap and ion cyclotron resonance. Anal. Chem. **88**, 12427–12436 (2016)
20. Konijnenberg, A., Bannwarth, L., Yilmaz, D., Koçer, A., Venien-Bryan, C., Sobott, F.: Top-down mass spectrometry of intact membrane protein complexes reveals oligomeric state and sequence information in a single experiment. Protein Sci. **24**, 1292–1300 (2015)
21. Haberger, M., Leiss, M., Heidenreich, A.-K., Pester, O., Hafenmair, G., Hook, M., Bonnington, L., Wegele, H., Haindl, M., Reusch, D., Bulau, P.: Rapid characterization of biotherapeutic proteins by size-exclusion chromatography coupled to native mass spectrometry. MAbs. **8**, 331–339 (2016)
22. Muneeruddin, K., Thomas, J.J., Salinas, P.A., Kaltashov, I.A.: Characterization of small protein aggregates and oligomers using size exclusion chromatography with online detection by native electrospray ionization mass spectrometry. Anal. Chem. **86**, 10692–10699 (2014)
23. Melani, R.D., Seckler, H.S., Skinner, O.S., Do Vale, L.H., Catherman, A.D., Havugimana, P.C., Valle de Sousa, M., Domont, G.B., Kelleher, N.L., Compton, P.D.: CN-GELFrEE - clear native gel-eluted liquid fraction entrapment electrophoresis. J. Vis. Exp. (108) 53597 (2016)
24. Debaene, F., Bœuf, A., Wagner-Rousset, E., Colas, O., Ayoub, D., Corvaïa, N., Van Dorsselaer, A., Beck, A., Cianférani, S.: Innovative native MS methodologies for antibody drug conjugate characterization: high resolution native MS and IM-MS for average DAR and DAR distribution assessment. Anal. Chem. **86**, 10674–10683 (2014)
25. Shen, X., Kou, Q., Guo, R., Yang, Z., Chen, D., Liu, X., Hong, H., Sun, L.: Native proteomics in discovery mode using size-exclusion chromatography–capillary zone electrophoresis–tandem mass spectrometry. Anal. Chem. **90**, 10095–10099 (2018)
26. Cleary, S.P., Li, H., Bagal, D., Loo, J.A., Campuzano, I.D.G., Prell, J.S.: Extracting charge and mass information from highly congested mass spectra using Fourier-domain harmonics. J. Am. Soc. Mass Spectrom. **29**, 2067–2080 (2018)
27. Marty, M.T., Baldwin, A.J., Marklund, E.G., Hochberg, G.K.A., Benesch, J.L.P., Robinson, C.V.: Bayesian deconvolution of mass and ion mobility spectra: from binary interactions to polydisperse ensembles. Anal. Chem. **87**, 4370–4376 (2015)
28. Huttlin, E.L., Ting, L., Bruckner, R.J., Gebreab, F., Gygi, M.P., Szpyt, J., Tam, S., Zarraga, G., Colby, G., Baltier, K., Dong, R., Guarani, V., Vaites, L.P., Ordureau, A., Rad, R., Erickson, B.K., Wühr, M., Chick, J., Zhai, B., Kolippakkam, D., Mintseris, J., Obar, R.A., Harris, T., Artavanis-Tsakonas, S., Sowa, M.E., De Camilli, P., Paulo, J.A., Harper, J.W., Gygi, S.P.: The BioPlex network: a systematic exploration of the human interactome. Cell. **162**, 425–440 (2015)
29. DeHart, C.J., Fellers, R.T., Fornelli, L., Kelleher, N.L., Thomas, P.M.: Bioinformatics Analysis of Top-Down Mass Spectrometry Data with ProSight Lite. In: Wu, C.H., Arighi, C.N., Ross, K.E. (eds.) Protein Bioinformatics. Methods in Molecular Biology, vol. 1558. Humana Press, New York, NY (2017)
30. Fellers, R.T., Greer, J.B., Early, B.P., Yu, X., LeDuc, R.D., Kelleher, N.L., Thomas, P.M.: ProSight lite: graphical software to analyze top-down mass spectrometry data. Proteomics. **15**, 1235–1238 (2015)
31. Marshall, A.G., Hendrickson, C.L.: High-resolution mass spectrometers. Annu. Rev. Anal. Chem. **1**, 579–599 (2008)
32. Ens, W., Standing, K.G.: Hybrid Quadrupole/Time-of-Flight Mass Spectrometers for Analysis of Biomolecules. Methods Enzymol. **402**, 49–78 (2005)
33. Snijder, J., Heck, A.J.R.: Analytical approaches for size and mass analysis of large protein assemblies. Annu. Rev. Anal. Chem. **7**, 43–64 (2014)
34. Kozlovski, V.I., Donald, L.J., Collado, V.M., Spicer, V., Loboda, A.V., Chernushevich, I.V., Ens, W., Standing, K.G.: A TOF mass spectrometer for the study of noncovalent complexes. Int. J. Mass Spectrom. **308**, 118–125 (2011)
35. Sobott, F., Hernandez, H., McCammon, M.G., Tito, M.A., Robinson, C.V.: A tandem mass spectrometer for improved transmission and analysis of large macromolecular assemblies. Anal. Chem. **74**, 1402–1407 (2002)
36. van den Heuvel, R.H.H., van Duijn, E., Mazon, H., Synowsky, S.A., Lorenzen, K., Versluis, C., Brouns, S.J.J., Langridge, D., van der Oost, J., Hoyes, J., Heck, A.J.R.: Improving the performance of a quadrupole time-of-flight instrument for macromolecular mass spectrometry. Anal. Chem. **78**, 7473–7483 (2006)
37. Zubarev, R.A., Makarov, A.: Orbitrap mass spectrometry. Anal. Chem. **85**, 5288–5296 (2013)
38. Rose, R.J., Damoc, E., Denisov, E., Makarov, A., Heck, A.J.: High-sensitivity Orbitrap mass analysis of intact macromolecular assemblies. Nat. Methods. **9**, 1084–1086 (2012)
39. Jhingree, J.R., Bellina, B., Pacholarz, K.J., Barran, P.E.: Charge mediated compaction and rearrangement of gas-phase proteins: a case study considering two proteins at opposing ends of the structure-disorder continuum. J. Am. Soc. Mass Spectrom. **28**, 1450–1461 (2017)
40. Laszlo, K.J., Bush, M.F.: Effects of charge state, charge distribution, and structure on the ion mobility of protein ions in helium gas: results from trajectory method calculations. J. Phys. Chem. A. **121**, 7768–7777 (2017)
41. Ruotolo, B.T., Hyung, S.-J., Robinson, P.M., Giles, K., Bateman, R.H., Robinson, C.V.: Ion mobility–mass spectrometry reveals long-lived, unfolded intermediates in the dissociation of protein complexes. Angew. Chem. Int. Ed. **46**, 8001–8004 (2007)
42. Wongkongkathep, P., Han, J.Y., Choi, T.S., Yin, S., Kim, H.I., Loo, J.A.: Native top-down mass spectrometry and ion mobility MS for characterizing the cobalt and manganese metal binding of α-synuclein protein. J. Am. Soc. Mass Spectrom. **29**, 1870–1880 (2018)
43. Caravatti, P., Allemann, M.: The 'infinity cell': a new trapped-ion cell with radiofrequency covered trapping electrodes for Fourier transform ion cyclotron resonance mass spectrometry. Org. Mass Spectrom. **26**, 514–518 (1991)
44. Li, H., Wolff, J.J., Van Orden, S.L., Loo, J.A.: Native top-down electrospray ionization-mass spectrometry of 158 kDa protein complex by high-resolution Fourier transform ion cyclotron resonance mass spectrometry. Anal. Chem. **86**, 317–320 (2014)
45. van de Waterbeemd, M., Fort, K.L., Boll, D., Reinhardt-Szyba, M., Routh, A., Makarov, A., Heck, A.J.: High-fidelity mass analysis unveils heterogeneity in intact ribosomal particles. Nat. Methods. **14**, 283–286 (2017)
46. Snijder, J., Uetrecht, C., Rose, R.J., Sanchez-Eugenia, R., Marti, G.A., Agirre, J., Guérin, D.M.A., Wuite, G.J.L., Heck, A.J.R., Roos, W.H.: Probing the biophysical interplay between a viral genome and its capsid. Nat. Chem. **5**, 502 (2013)
47. van de Waterbeemd, M., Tamara, S., Fort, K.L., Damoc, E., Franc, V., Bieri, P., Itten, M., Makarov, A., Ban, N., Heck, A.J.R.: Dissecting ribosomal particles throughout the kingdoms of life using advanced hybrid mass spectrometry methods. Nat. Commun. **9**, 2493 (2018)
48. Haverland, N.A., Skinner, O.S., Fellers, R.T., Tariq, A.A., Early, B.P., LeDuc, R.D., Fornelli, L., Compton, P.D., Kelleher, N.L.: Defining gas-phase fragmentation propensities of intact proteins during native top-down mass spectrometry. J. Am. Soc. Mass Spectrom. **28**, 1203–1215 (2017)
49. Zhou, M., Wysocki, V.H.: Surface induced dissociation: dissecting noncovalent protein complexes in the gas phase. Acc. Chem. Res. **47**, 1010–1018 (2014)
50. Brodbelt, J.S.: Photodissociation mass spectrometry: new tools for characterization of biological molecules. Chem. Soc. Rev. **43**, 2757–2783 (2014)
51. Lermyte, F., Valkenborg, D., Loo, J.A., Sobott, F.: Radical solutions: principles and application of electron-based dissociation in mass spectrometry-based analysis of protein structure. Mass Spectrom. Rev. **37**, 750–771 (2018)
52. Hewitt, J.A., Brown, L.L., Murphy, S.J., Grieder, F., Silberberg, S.D.: Accelerating biomedical discoveries through rigor and transparency. ILAR J. **58**, 115–128 (2017)
53. Landis, S.C., Amara, S.G., Asadullah, K., Austin, C.P., Blumenstein, R., Bradley, E.W., Crystal, R.G., Darnell, R.B., Ferrante, R.J., Fillit, H., Finkelstein, R., Fisher, M., Gendelman, H.E., Golub, R.M., Goudreau, J.L., Gross, R.A., Gubitz, A.K., Hesterlee, S.E., Howells, D.W., Huguenard, J., Kelner, K., Koroshetz, W., Krainc, D., Lazic, S.E., Levine, M.S., Macleod, M.R., McCall, J.M., Moxley, R.T., Narasimhan, K., Noble, L.J., Perrin, S., Porter, J.D., Steward, O., Unger, E., Utz, U., Silberberg, S.D.: A call for transparent reporting to optimize the predictive value of preclinical research. Nature. **490**, 187–191 (2012)

54. Hartshorne, J.K., Schachner, A.: Tracking replicability as a method of post-publication open evaluation. Front. Comput. Neurosci. **6**, 8 (2012)
55. Ioannidis, J.P.A., Khoury, M.J.: Improving validation practices in "omics" research. Science. **334**, 1230–1232 (2011)
56. Kirshenbaum, N., Michaelevski, I., Sharon, M.: Analyzing large protein complexes by structural mass spectrometry. J. Vis. Exp. (40) 1954 (2010)
57. Laganowsky, A., Reading, E., Hopper, J.T.S., Robinson, C.V.: Mass spectrometry of intact membrane protein complexes. Nat. Protoc. **8**, 639 (2013)
58. van Dyck, J.F., Konijnenberg, A., Sobott, F.: Native Mass Spectrometry for the Characterization of Structure and Interactions of Membrane Proteins. In: Lacapere, J.-J. (ed.) Membrane Protein Structure and Function Characterization. Methods Mol Biol, vol. 1635. Humana Press, New York, NY (2017)
59. Thompson, N.J., Rosati, S., Heck, A.J.: Performing native mass spectrometry analysis on therapeutic antibodies. Methods. **65**, 11–17 (2014)
60. Perry, R.H., Cooks, R.G., Noll, R.J.: Orbitrap mass spectrometry: instrumentation, ion motion and applications. Mass Spectrom. Rev. **27**, 661–699 (2008)
61. Konermann, L.: Addressing a common misconception: ammonium acetate as neutral pH "buffer" for native electrospray mass spectrometry. J. Am. Soc. Mass Spectrom. **28**, 1827–1835 (2017)
62. Liu, C.C., Zhang, J., Dovichi, N.J.: A sheath-flow nanospray interface for capillary electrophoresis/mass spectrometry. Rapid Commun. Mass Spectrom. **19**, 187–192 (2005)
63. Hao, Z., Zhang, T., Xuan, Y., Wang, H., Qian, J., Lin, S., Chen, J., Horn, D.M., Argoti, D., Beck, A., Cianférani, S., Bennett, P., Miller, K., Makarov, A.: Intact Antibody Characterization Using Orbitrap Mass Spectrometry. State-of-the-Art and Emerging Technologies for Therapeutic Monoclonal Antibody Characterization Volume 3. Defining the Next Generation of Analytical and Biophysical Techniques, American Chemical Society. **1202**, 289–315 (2015)
64. Rosati, S., Yang, Y., Barendregt, A., Heck, A.J.: Detailed mass analysis of structural heterogeneity in monoclonal antibodies using native mass spectrometry. Nat. Protoc. **9**, 967–976 (2014)
65. Schachner, L., Han, G., Dillon, M., Zhou, J., McCarty, L., Ellerman, D., Yin, Y., Spiess, C., Lill, J.R., Carter, P.J., Sandoval, W.: Characterization of chain pairing variants of bispecific IgG expressed in a single host cell by high-resolution native and denaturing mass spectrometry. Anal. Chem. **88**, 12122–12127 (2016)
66. Zhang, H., Cui, W., Gross, M.L.: Mass spectrometry for the biophysical characterization of therapeutic monoclonal antibodies. FEBS Lett. **588**, 308–317 (2014)
67. Saito, R., Sato, T., Ikai, A., Tanaka, N.: Structure of bovine carbonic anhydrase II at 1.95 A resolution. Acta Crystallogr. D Biol. Crystallogr. **60**, 792–795 (2004)
68. Jörnvall, H.: The primary structure of yeast alcohol dehydrogenase. Eur. J. Biochem. **72**, 425–442 (1977)
69. Li, H., Wongkongkathep, P., Van Orden, S.L., Loo, R.R.O., Loo, J.A.: Revealing ligand binding sites and quantifying subunit variants of noncovalent protein complexes in a single native top-down FTICR MS experiment. J. Am. Soc. Mass Spectrom. **25**, 2060–2068 (2014)
70. Holland, M.J., Holland, J.P., Thill, G.P., Jackson, K.A.: The primary structures of two yeast enolase genes. Homology between the 5′ noncoding flanking regions of yeast enolase and glyceraldehyde-3-phosphate dehydrogenase genes. J. Biol. Chem. **256**, 1385–1395 (1981)